Distributed particle filter for bearing-only tracking

Jun Ye Yu

January 9, 2018

1 Introduction

In this report we present four distributed particle filters for single-target bearing-only tracking. The first filter factorizes the joint log-likelihood function using six global sufficient statistics that can be computed using distributed summation. The second filter uses likelihood consensus to approximate the measurement function with a number of basis functions. The third filter constructs a graph over all particles and the Eigenvectors of the resulting Laplacian matrix are used to encode the particle log-likelihood using a minimal number of coefficients. Finally, the fourth filter groups all particles into clusters and computes the cluster joint likelihood. The individual particle weights are then recovered via convex minimization. For the remainder of the report, we refer to the four particle filters as **CSSpf** [1], **LCpf** [2], **LApf** [3] and **Clusterpf** [4] respectively. We also include the centralized *bootstrap particle filter* (**BSpf**) as baseline.

The remainder of the report is organized as follows. Sec. 2 defines the tracking problem. Sec. 3 presents the particle filters. Sec. 3.4 compares the filters' performance and Sec. 5 concludes the report.

2 Problem statement

A network of S sensors collaboratively track a single moving target over time. The sensors have fixed position $[x_s, y_s], s = 1...S$. The target state at time k is modeled as $X(k) = [x_t(k), y_t(k), \dot{x}_t(k), \dot{y}_t(k)]$ where $x_t(k)$, $y_t(k)$ are the target position and $\dot{x}_t(k)$, $\dot{y}_t(k)$ are its velocity.

At time k, the target transitions to new state $X(k)$ with probability $f(X(k)|X(k-1))$ which depends on the target dynamic model. Each sensor s also receives a noisy measurement $z_s(k)$ with likelihood $f(z_s(k)|H_s(X(k))$ where $H_s(\cdot)$ is the (possibly sensor-dependent) measurement function. The sensors have unity target detection probability and receive no clutter measurement.

In this report, we focus on bearing-only tracking. Each sensor receive a bearing measurement corrupted by additive zero-mean Gaussian noise, and has the following measurement model:

$$H_s(X) = \arctan 2\left(\frac{x_t - x_s}{y_t - y_s}\right) + \eta_s \tag{1}$$

where $\eta_s \sim \mathcal{N}(0, \sigma_s)$ is the measurement noise.

3 Distributed particle filters for bearing-only tracking

In a particle filter, the posterior target density is modeled using a set of N particles with normalized weights $\{X_i(k), w_i(k)\}_{i=1}^N$, and the objective is to recursively estimate the posterior particle weights. This in turn

requires the computation of joint log-likelihood:

$$w_i(k) \propto \log(f(z_1(k), ...z_S(k)|X_i(k))) \propto \sum_{s=1}^{S} \frac{-(z_s - H_s(X))^2}{2\sigma_s^2}$$
$$= \sum_{s=1}^{S} \frac{-(z_s)^2 - H_s(X)^2 + 2z_s H_s(X)}{2\sigma_s^2} \quad (2)$$

where measurements from different sensors are assumed to be conditionally independent given the target state.

For the remainder of this section, we present four distributed particle filters which compute the joint log-likelihood in different manners. We omit time step indice k where there is no ambiguity. For convenience of notation, let $\gamma_s = [\log(f(z_s|X_1), ... \log(f(z_s|x_N))]^T$ denote the column vector containing the log-likelihoods of all N particles at sensor s. Similarly, let $\gamma = [\log(f(z_1, ..., z_S|X_1), ... \log(f(z_1, ..., z_S|x_N))]^T$ denote the column vector of joint log-likelihood.

3.1 Constraint sufficient statistics particle filter

In the CSSpf, the likelihood function is approximated as follows:

$$\log(f(z_s|X) \approx \sum_{j=1}^{6} G_{s,j} F_j(X) \quad (3)$$

$$G_{s,1} = (Z_{s,\theta})^2/R_\theta$$
$$G_{s,2} = \cos^2(Z_{s,\theta})/R_\theta$$
$$G_{s,3} = \sin^2(Z_{s,\theta})/R_\theta$$
$$G_{s,4} = \sin(Z_{s,\theta})\cos(Z_{s,\theta})/R_\theta$$
$$G_{s,5} = Z_{s,\theta}\cos(Z_{s,\theta})/R_\theta$$
$$G_{s,6} = Z_{s,\theta}\sin(Z_{s,\theta})/R_\theta$$
$$Z_{s,\theta} = y_s \sin(z_s) - x_s \cos(z_s)$$
$$R_\theta = E((x_t - x_s)^2 + (y_t - y_s)^2)(1 - \exp^{-2\sigma_\theta^2})/2$$

$$F_1(X) = 1$$
$$F_2(X) = x_t^2$$
$$F_3(X) = y_t^2$$
$$F_4(X) = -2x_t y_t$$
$$F_5(X) = 2x_t$$
$$F_6(X) = -2y_t$$

The functions $F_j(X)$ depend only on X and are known to all sensors. The sufficient statistics $G_{s,j}$ depend only on local information from sensor s. In other words, we approximate the log-likelihood function by the combination of six basis functions $F_j(X)$ with corresponding coefficients $G_{s,j}$.

This formulation leads to the following approximate log-likelihood function

$$\log(f(z_1, ..., z_S|X) \approx \sum_{j=1}^{6} F_j(X) \left(\sum_{s=1}^{S} G_{s,j} \right) \quad (4)$$

where the summation terms $\left(\sum_{s=1}^{S} G_{s,j}\right)$ can be interpreted as the global sufficient statistics. These global sufficient statistics can be computed in a distributed manner by running six consensus algorithms in parallel. Note that the per-sensor communication overhead of CSSpf is constant since there are only six statistics to aggregate regardless of number of particles.

The CSSpf is derived based on LCpf and the six basis functions are specifically tailored for bearing-only tracking. For other measurement model, re-derivation of the filter is required.

3.2 Likelihood consensus particle filter

In LCpf, we approximate the measurement function as follows:

$$\hat{H}_s(X) = \sum_{j=1}^{J} \alpha_{s,j}\beta_j(X) \tag{5}$$

where $\beta_j(X)$ is the j^{th} sensor-independent basis function and $\alpha_{s,j}$ is the corresponding coefficient that encompasses all the local information of sensor s.

Plugging Eq. (5) into Eq. (2) yields

$$\begin{aligned}
\log(f(z_1,...z_S|X)) &\propto -\sum_{s=1}^{S}\frac{(z_s)^2}{2\sigma_s^2} - \sum_{s=1}^{S}\frac{\left(\sum_{j=1}^{J}\alpha_{s,j}\beta_j(X)\right)^2}{2\sigma_s^2} + \sum_{s=1}^{S}\frac{z_s\sum_{j=1}^{J}\alpha_{s,j}\beta_j(X)}{\sigma_s^2} \\
&= -\frac{\sum_{s=1}^{s}(z_s)^2}{2\sigma_s^2} - \sum_{j_1=1}^{J}\sum_{j_2=1}^{J}\frac{\sum_{s=1}^{s}\alpha_{s,j_1}\alpha_{s,j_2}\beta_{j_1}(X)\beta_{j_2}(X)}{2\sigma_s^2} + \sum_{j=1}^{J}\frac{\sum_{s=1}^{S}z_s\alpha_{s,j}\beta_j(X)}{\sigma_s^2} \\
&= -\frac{\sum_{s=1}^{S}(z_s)^2}{2\sigma_s^2} - \sum_{m=1}^{M}B_m(X)\left(\sum_{s=1}^{S}\frac{A_{s,m}}{2\sigma_s^2}\right) + \sum_{j=1}^{J}\beta_j(X)\left(\sum_{s=1}^{S}\frac{z_s\alpha_{s,j}}{\sigma_s^2}\right)
\end{aligned} \tag{6}$$

where, for the last equality, we employ a suitable mapping $m \to (j_1, j_2)$, $M = J^2$, $B_m(X) = \beta_{j_1}(X)\beta_{j_2}(X)$ and $A_{s,m} = \alpha_{s,j_1}\alpha_{s,j_2}$.

Eq. (6) suggests that the joint log-likelihood can be constructed using $M + J$ consensus algorithms in parallel to compute the global sufficient statistics $\sum_{s=1}^{S}\frac{A_{s,m}}{2\sigma_s^2}$ and $\sum_{s=1}^{S}\frac{z_s\alpha_{s,j}}{\sigma_s^2}$. The first term in Eq. (6) is constant and independent of X and can thus be ignored.

We now describe how to compute the coefficients $\alpha_{s,j}$ using the least-square approach. Given the N particles X_i, we construct the $N \times J$ matrix Φ as follows:

$$\Phi = \begin{pmatrix} \beta_1(X_1) & ... & \beta_J(X_1) \\ ... & ... & ... \\ \beta_1(X_N) & ... & \beta_J(X_N) \end{pmatrix} \tag{7}$$

For each sensor s, we also construct the following column vector

$$\Lambda_s = [H_s(X_1), ...H_s(X_N)]^T \tag{8}$$

where T denotes the transpose operation.

We seek a set of coefficients $\alpha_s = [\alpha_{s,1}, ...\alpha_{s,J}]^T$ such that the approximation error $\Lambda_s - \Phi\alpha_s$ is minimized. Using the least-square approach yields

$$\alpha_s = (\Phi^T\Phi)^{-1}\Phi^T\Lambda_s \tag{9}$$

We note that the LCpf is not restricted to approximating the measurement function only. The same approach can be applied to estimate the particle log-likelihoods directly as in the case of CSSpf. The communication overhead per sensor depends directly on the number of coefficients which may in turn depend on the number of particles and other factors.

3.3 Laplacian approximation particle filter

In LApf, we consider each particle X_i a vertex on a graph. The *Delaunay triangulation* (DT) on these particles is used to construct a graph. The resulting Laplacian matrix is used to construct a transformation that allows particle log-likelihoods to be represented using a minimal number of coefficients.

Let L denote the Laplacian matrix of the DT graph with eigenvalue decomposition $L = E^T\Lambda E$. The eigenvectors are used as the basis of transformation of particle log-likelihoods into Laplacian domain. Using

all N eigenvectors is obviously counterproductive since we incur the computational cost of eigendecomposition and achieve no reduction in communication overhead (i.e., we still have to aggregate N coefficients).

Assume that $m \leq N$ eigenvectors are used as the basis of transformation and let E_m denote the resulting matrix. We compute the local coefficients at sensor s as follows:

$$\alpha_s = E_m^T \gamma_s \tag{10}$$

The global coefficients are the summation of local coefficients across all S sensors: $\alpha = \sum_s \alpha_s$. Finally, the approximate joint log-likelihood can be computed as follows:

$$\hat{\gamma} = E_m \alpha = E_m \sum_s \alpha_s \tag{11}$$

Since the particle log-likelihoods can be considered as a smooth signal over the graph (i.e., particles close to each other have similar log-likelihoods), most of their energy should be concentrated in the coefficients corresponding to lower frequency basis vectors. In other words, we should retain the m eigenvectors corresponding to the m smallest eigenvalues.

We note that LApf is similar to CSSpf in that both filters encode the particle log-likelihoods directly using a minimal number of coefficients.

3.4 Clustering particle filter

In Clusterpf, the particles are grouped into N_c clusters based on their position. The sensors reach consensus on the cluster log-likelihoods rather than individual particle log-likelihoods. For $c \ll N$, significant reduction in communication overhead can be achieved.

We follow the approach in [2]. The log-likelihood of each cluster is equal to the aggregate log-likelihood of its constituent particles. Let γ^c denote the joint log-likelihood of the clusters after consensus. Let C denote the $N_c \times N$ cluster assignment matrix where $C(i,j) = 1$ denotes that particle j belongs to cluster i.

In order to recover the individual particle joint log-likelihoods γ, we again construct the K-nearest-neighbor graph, compute the Laplacian matrix L, and then solve the following convex minimization problem:

$$\begin{aligned} \underset{\gamma}{\text{minimize}} \quad & \gamma^T L \gamma \\ \text{subject to} \quad & C\gamma = \gamma^c \end{aligned}$$

In other words, we seek to assign particle log-likelihood values that are smooth with respect to particle proximity while ensuring the aggregate particle values are equal to the cluster value.

4 Performance evaluation

4.1 Simulation setup

In this section, we evaluate and compare the performance of the four filters presented in Sec. 3. We also include a centralized bootstrap filter as baseline. We construct a network of $S = 9$ sensors in a square grid over a 75km $\times$ 75km area and track a target traveling in counter-clockwise direction over 50 time steps. The sensors remain static over time. Fig. 1 shows the target trajectory and sensor positions.

The target state evolves over time following a discrete-time model:

$$X(k+1) = F(X(k)) + \xi(k) \tag{12}$$

where $F(X(k))$ is the dynamic model and $\xi(k)$ is the zero-mean Gaussian process noise. The simulated target randomly switches between two different motion models: constant velocity with probability $P_{cv} = 0.05$ and coordinated turn with probability $1 - P_{cv} = 0.95$.

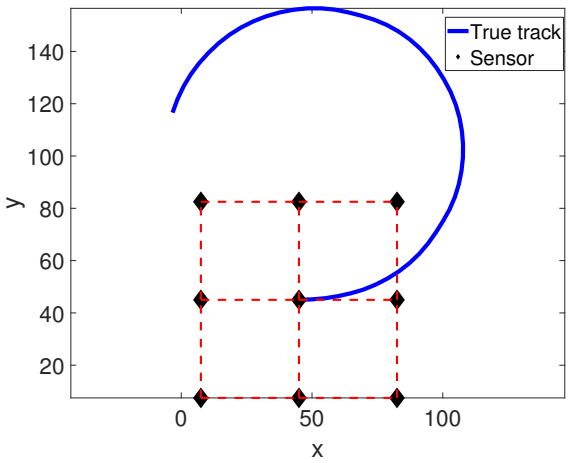

Figure 1: Target trajectory (blue curve) and sensor positions (black diamond). Sensors connected by red dashed lines are within broadcast range of each other.

For constant velocity, we have

$$F(X(k)) = \begin{matrix} 1 & 0 & 1 & 0 \\ 0 & 1 & 0 & 1 \\ 0 & 0 & 1 & 0 \\ 0 & 0 & 0 & 1 \end{matrix} \tag{13}$$

For coordinated turn, we have

$$F(X(k)) = \begin{bmatrix} 1 & 0 & \frac{\sin(\Omega)}{\Omega(k)} & -\frac{1-\cos(\Omega(k))}{\Omega(k)} \\ 0 & 1 & \frac{1-\cos(\Omega(k))}{\Omega(k)} & \frac{\sin(\Omega(k))}{\Omega(k)} \\ 0 & 0 & \cos(\Omega(k)) & -\sin(\Omega(k)) \\ 0 & 0 & \sin(\Omega(k)) & \cos(\Omega(k)) \end{bmatrix} \tag{14}$$

where $\Omega(k)$ is the turning rate

$$\Omega(k) = \frac{a}{\sqrt{\dot{x}^2(k) + \dot{y}^2(k)}} \tag{15}$$

with $a \in \mathbb{R}$ being the maneuver acceleration parameter.

All sensors receive noisy bearing measurements (in radians) from the target.

$$H_s(X(k)) = \arctan 2 \left(\frac{x_t - x_s}{y_t - y_s} \right) + \eta(k) \tag{16}$$

The process and measurement noises $\xi(k)$ and $\eta(k)$ have covariance matrices Q and R respectively.

$$Q = \sigma_a^2 \begin{bmatrix} \frac{1}{3} & 0 & \frac{1}{2} & 0 \\ 0 & \frac{1}{3} & 0 & \frac{1}{2} \\ \frac{1}{2} & 0 & 1 & 0 \\ 0 & \frac{1}{2} & 0 & 1 \end{bmatrix} \tag{17}$$

$$R = \sigma_\theta^2 \tag{18}$$

where $\sigma_a = 10^{-4}$, and $\sigma_\theta = 0.0873$ rad $= 5$ degree.

4.2 Algorithm setup

All particle filters use a total of $N = 500$ particles. At time step 1, we generate the initial particles using the true target state: $X_i(1) \sim \mathcal{N}(X(1), R_{\text{initial}})$ with $R_{\text{initial}} = \text{diag}([0.5^2, 0.5^2, 0.05^2, 0.05^2])$.

For LCpf, we use a set of basis functions involving all permutations of $x_t^i y_t^j$ with $0 \leq i, j \leq d$ where d is some user-specified max degree. For $d = 2$, the basis functions would be

$$\begin{aligned}\beta_1(X) &= x_t^0 y_t^0 = 1 \\ \beta_2(X) &= x_t^0 y_t^1 = y_t \\ &\cdots \\ \beta_9(X) &= x_t^2 y_t^2\end{aligned}$$

Note that, due to our choice of basis functions, all particles must remain synchronized across all sensors as in the case of LApf and Clusterpf.

For LApf, we construct a DT graph and retain $m < N$ eigenvectors as the basis of Laplacian transformation. For Clusterpf, all particles are grouped into C clusters and a DT graph is constructed to recover individual particle weights.

Finally, the random number generators are synchronized to ensure that the particles remain the same across sensors. Distributed summation is performed using gossip algorithms. At each time step, we perform $NGossip$ gossip iterations. At each gossip iteration t, each sensor i broadcasts its local values $G_i(t)$, receives broadcasts from its neighbors, and then updates its local values as a weighted aggregate:

$$G_i(t+1) = w_{ii} G_i(t) + \sum_{j \in N_i} w_{ij} G_j(t) \tag{19}$$

$$w_{ij} = \begin{cases} \frac{1}{1+max(d_i, d_j)} & j \in N_i \\ 1 - \sum_{j \in N_i} w_{ij} & i = j \\ 0 & j \notin N_i \end{cases} \tag{20}$$

where N_i denotes the set of neighboring sensors of sensor i and Metropolis weight is used for the update. After a total of $NGossip$ iterations, a max consensus algorithm is run to ensure all sensors obtain the same values.

In our codes, we do not implement a loop for each gossip iteration. Instead we define an update matrix W where $W(i, j) = w_{ij}$. Therefore, given initial values $G(1) = [G_1(1), ..., G_S(1)]^T$, the final values can be easily computed as

$$G(NGossip) = W^{NGossip} G(1) \tag{21}$$

Since the sensors remain static over time in our simulation, W remains static and a quick computation shows that $W_{final} = W^{31}$ is sufficiently close to an averaging matrix (i.e. $W_{final}(i, j) = 1/S$).

In the remainder of the section, we run a number of Monte Carlo simulations to evaluate the performance of individual algorithms. The track remains the same in each trial; but the measurements differ. We evaluate the algorithms' performances using three criterion: *root mean squared error* (RMSE) of position estimate, total runtime (from initialization to end of time step 50) and aggregate error ratio. The first two metrics are self-explanatory; so we will only explain the last one. Let G_{gossip} denote the vector of the approximate aggregate values computed using gossip and max consensus, and let G_{exact} denote the vector of exact aggregate values. We compute the ratio vector $|\frac{G_{gossip} - G_{exact}}{G_{exact}}|$ and report the average ratio. Ideally, for $NGossip$ approaching infinity, the ratio approaches 0 as the approximate aggregate value approaches the exact value.

4.3 Constraint sufficient statistics particle filter

Consider first CSSpf. Each sensor has a fixed communication overhead at each time step (i.e., broadcast $6NGossip$ scalars). We thus study the trade-off between communication overhead and tracking performance.

Fig. 2 shows the boxplots of RMSE, total runtime and aggregate error ratio with respect to number of gossip iterations and number of particles over 200 random trials. Each data point is averaged over all sensors and all time steps.

The RMSE is very high for $NGossip = 10$ which can be attributed to the gossip algorithms not converging in such few iterations and leading to high errors in the final aggregate values of the global sufficient statistics. For $NGossip \geq 20$ and $N \geq 100$, the RMSE is fairly constant and, at least for the given track, more gossip iterations and more particles do not yield significant improvement in tracking performance.

The runtime does not increase with higher $NGossip$ due to our implementation of the gossip algorithms. When N increases, the runtime increases as expected.

Finally, consider the aggregate error ratio. With increasing $NGossip$, the ratio decreases exponentially (note the log-scale of the Y-axis). For $NGossip = 10$, the gossip algorithms clearly have not converged and the error ratio can be as high as 10%. This explains the high RMSE values. For $NGossip = 20$, the ratio drops close to 0.02 which is low enough to yield adequate tracking performance. For higher values of $NGossip$, the ratio drops even further; although the tracking performance improvement is marginal at best. As N increases, the aggregate error ratio does not change significantly. This is to be expected since the number of sufficient statistics to be aggregated is constant and independent of the number of particles.

4.4 Likelihood consensus particle filter

The max degree d offers a trade-off between tracking performance and computational/communication overhead. Higher degree d generates more basis functions and should yield better approximation of the measurement model. On the other hand, more basis functions lead to more computation, more communication and longer runtime. In fact, the total number of basis functions grows exponentially with d (i.e., $O(d^2)$).

Fig. 3 shows the boxplots of RMSE and total runtime with respect to d. Note that, for this particular set of trials, all aggregates are computed exactly without gossiping. The runtime increases for higher d due to the additional computational overhead as expected. For all values of d, the RMSE is fairly consistent which suggests that additional basis functions from $d \geq 1$ do not improve the approximation of the measurement model $H(X_i)$ by any significant margin. To confirm our conjecture, we compute the following metric. Let $H_{true}(X_i)$ denote the true expected measurement of particle X_i and let $H_{approx}(X_i)$ denote the approximate value computed using the basis functions. We then compute the measurement model approximation error $|H_{exact}(X_i) - H_{approx}(X_i)|$ averaged over all particles, all sensors and all time steps. Fig. 4 shows the boxplot of average measurement model approximation error with respect to d. While the average error does fluctuate somewhat with respect to d, the error remains very small in all cases (less than 1 degree) compared to the standard deviation of measurement noise (5 degrees). These results suggest that $d = 1$ is sufficient to yield adequate tracking performance while minimizing computational overhead.

Fig. 5 shows the boxplots of RMSE, total runtime and aggregate error ratio with respect to number of gossip iterations and number of particles over 200 random trials for $d = 1$. Each data point is averaged over all time steps. For LCpf, a minimal of 40 gossip iterations are necessary to ensure adequate tracking performance. Furthermore, recall that, at $d = 1$, a total of 20 scalars needs to be aggregated across the network. In other words, the communication overhead of LCpf is 6 times that of CSSpf (thrice the scalars to aggregate and twice as many gossip iterations) to achieve similar tracking performance. If we compare Fig. 2(c) and Fig. 5(c), we note that CSSpf and LCpf exhibit very similar level of aggregate error ratios for the same $NGossip$. This suggests that LCpf is significantly more susceptible to error induced by distributed aggregation. On the other hand, LCpf requires only half the runtime of CSSpf.

4.5 Laplacian approximation particle filter

The LApf has one parameter of interest: m, the number of eigenvectors to encode the particle log-likelihoods. Fig. 6 shows the boxplots of RMSE, runtime and aggregate error ratio of LApf with respect to m and $NGossip$ for $N = 500$.

The RMSE is fairly stable for all values of $NGossip$ and m. This suggests two things. First, 6 Eigenvalues are sufficient to encode most information regarding the particle log-likelihood. Second, as few as 10

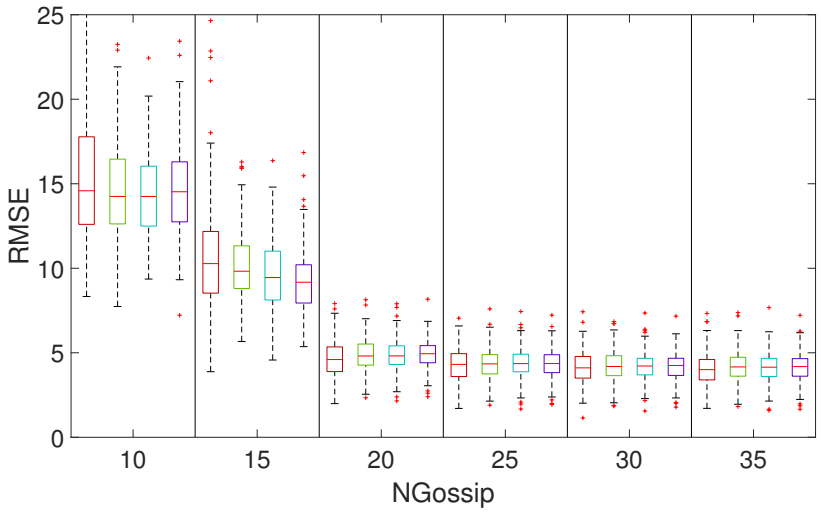

(a) RMSE

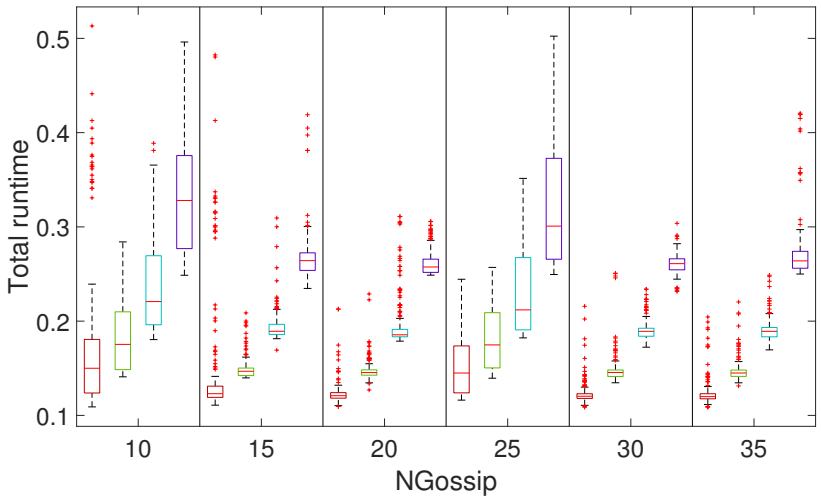

(b) total runtime

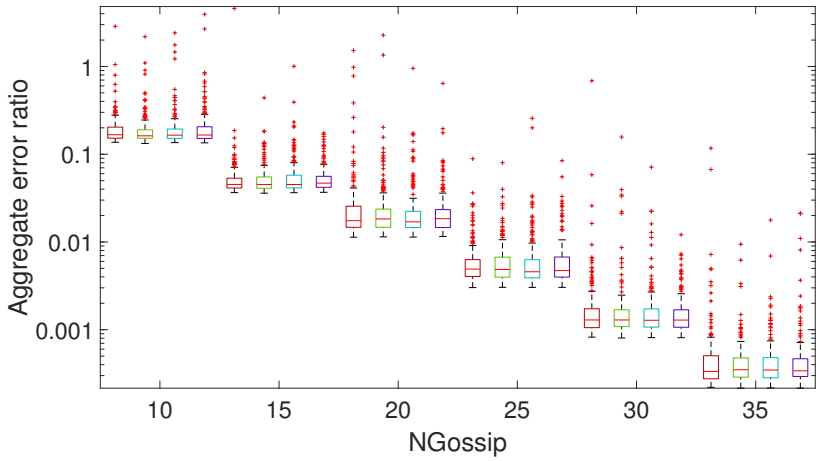

(c) total runtime

Figure 2: Boxplot of RMSE, runtime and aggregate error ratio of CSSpf with respect to $NGossip$ and N for 200 Monte Carlo trials. For each value of $NGossip$, from left to right, $N = 100, 250, 500, 1000$

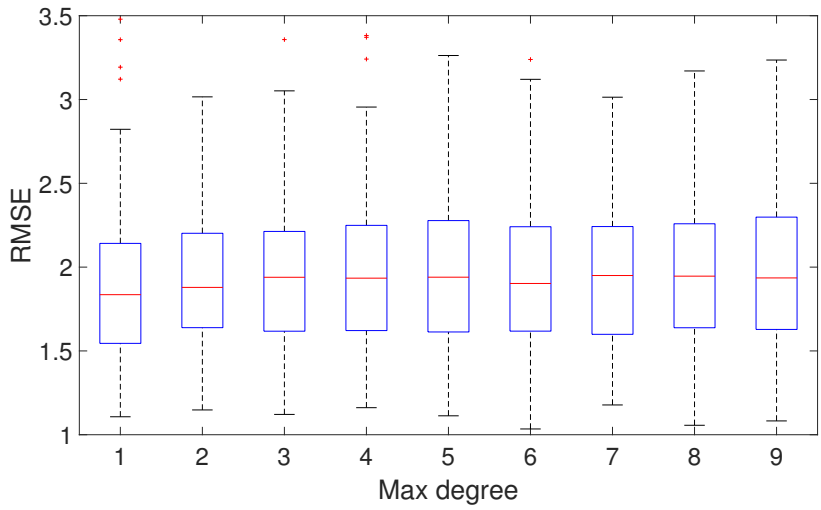

(a) RMSE

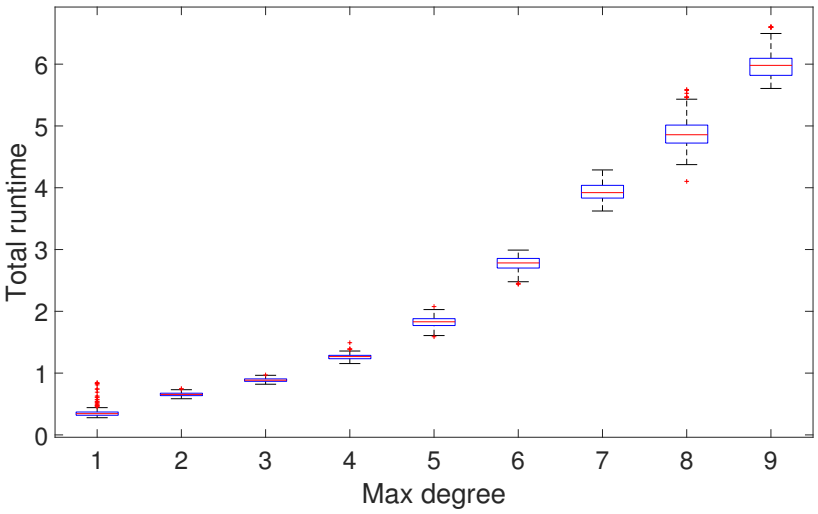

(b) total runtime

Figure 3: Boxplot of RMSE and total runtime of LCpf with respect to d. All aggregations are computed exactly without gossip.

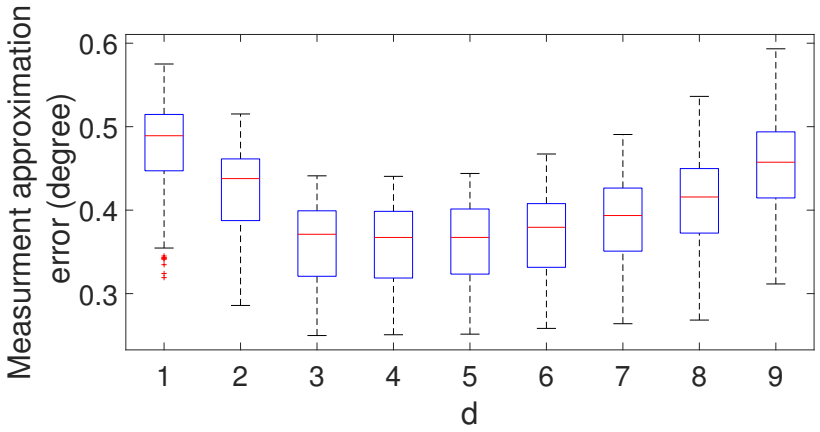

Figure 4: Boxplot of average measurement model approximation error with respect to d

gossip iterations per time step are sufficient to yield robust tracking performance. This strikes us as rather surprisingly since the average aggregate error of LApf is actually higher than that of LCpf and CSSpf for the same values of $NGossip$. This would suggest that LApf is surprisingly robust to error induced in distributed aggregation. Finally, the runtime is considerably higher than that of CSSpf and LCpf. The eigenvalue decomposition accounts for the bulk of the computational overhead which is independent of the values of $NGossip$ and m.

To confirm our conjecture regarding the choice of m, we compute the following metrics. Let $\hat{w}_i$ denote the approximate weight of particle X_i computed using the Laplacian transformations and let w_i denote the true particle weight. We compute and report the discrepancy $|\hat{w}_i - w_i|$ averaged over all particles and all time steps. Fig. 7 shows the boxplot of the weight discrepancy with respect to m. At $m = 6$, the average discrepancy is as low as $4e-4$. Increasing m to 100 only reduces the error by a factor of 3 while increasing the communication overhead by more than 15 times.

4.6 Cluster particle filter

The Clusterpf has two parameters of interest: number of clusters C and number of neighbors K for the graph construction. Table 1 shows the average RMSE of Clusterpf with respect to C and K. As C increases, the RMSE decreases. At $C = N = 1000$, the Clusterpf is equivalent to the centralized BSpf (assuming distributed summation without error) and the performance is independent of K. For any given value of C, as K increases, RMSE decreases. We note that these trends are similar to those shown in LApf. In fact, the parameter C serves the same role as m in LApf. Higher value of C requires higher communication overhead but reduces the approximation error of particle log-likelihoods. These results suggest that, as in the case of LApf, one may opt for a higher value of K in exchange for reduced communication overhead without significantly degrading tracking performance.

Table. 2 shows the total runtime of Clusterpf with respect to K and m. As C increases, so does the runtime with a huge spike after $C = 200$. A detailed breakdown of total runtime shows (Fig. **??**) that the computational overhead of particle clusters increases significantly with higher C. For a given value of C (Fig. **??**), increasing K leads to higher runtime which is caused by the higher computational overhead for nearest-neighbor graph construction and convex optimization.

4.7 Performance comparison between filters

In this section, we compare the filters against each other. We use the same test track from the previous section. Based on our results from previous sections, we use the following algorithm-specific parameters: $d = 1$ (LCpf), $K = 100$, $m = 6$ (LApf) and $K = 100$, $C = 6$ (Clusterpf). These parameters are chosen

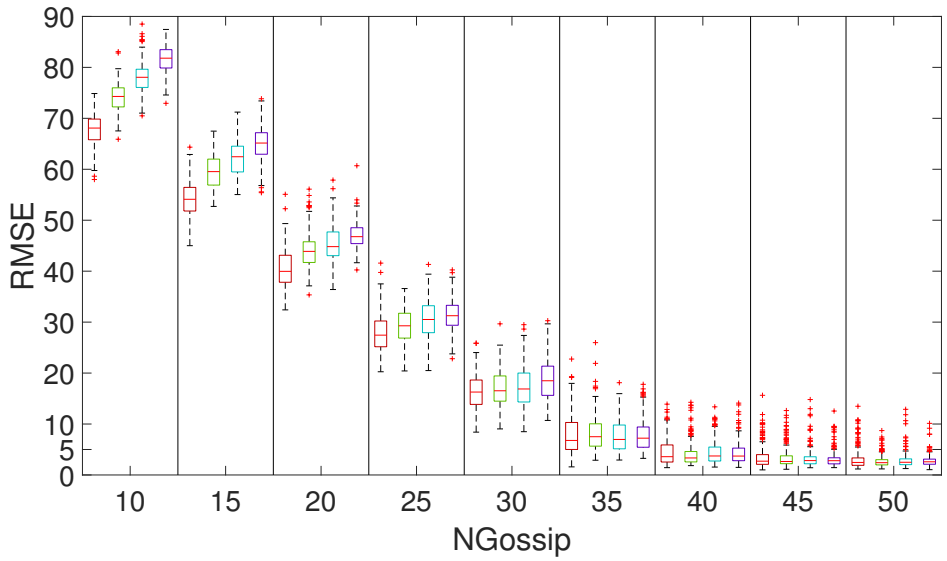

(a) RMSE

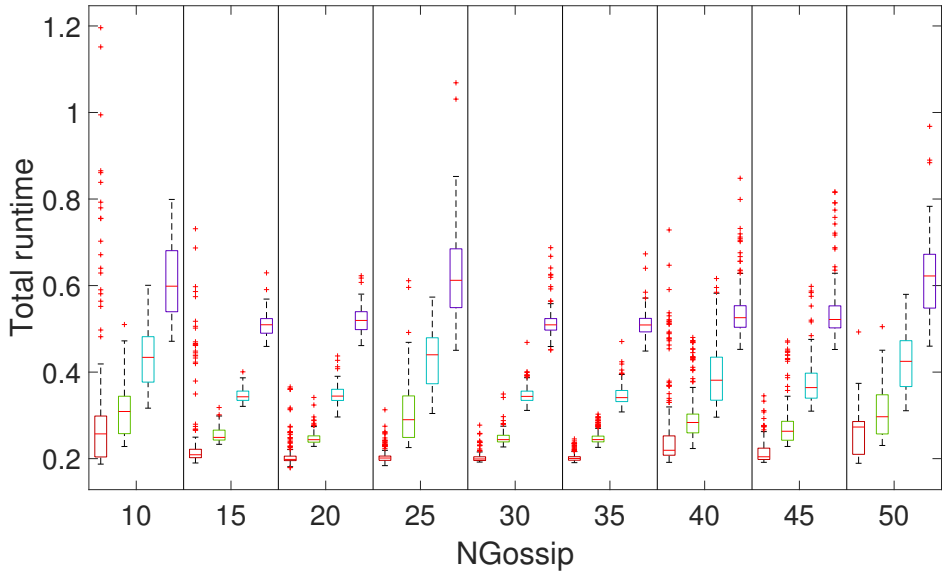

(b) total runtime

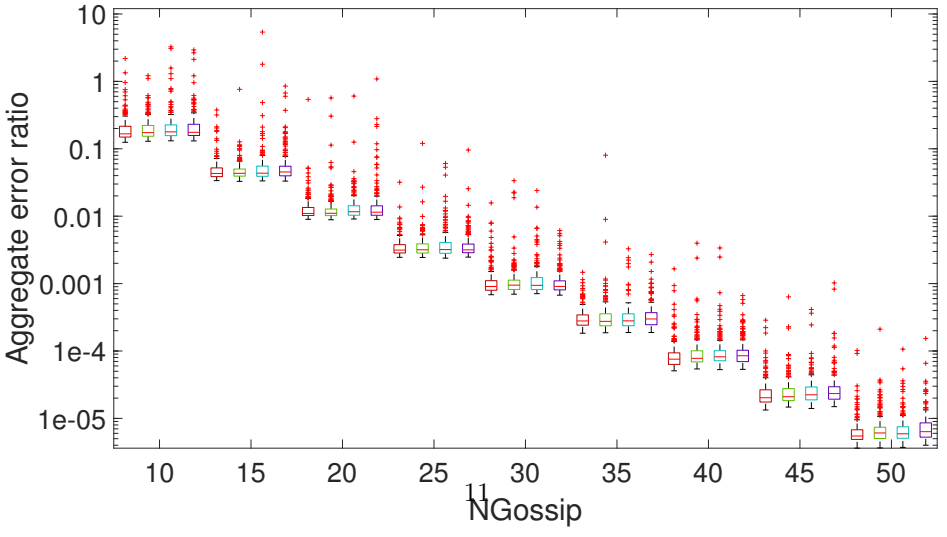

(c) total runtime

Figure 5: Boxplot of RMSE, runtime and aggregate error ratio of LCpf with respect to $NGossip$ and N for 200 Monte Carlo trials. For each value of $NGossip$, from left to right, $N = 100, 250, 500, 1000$

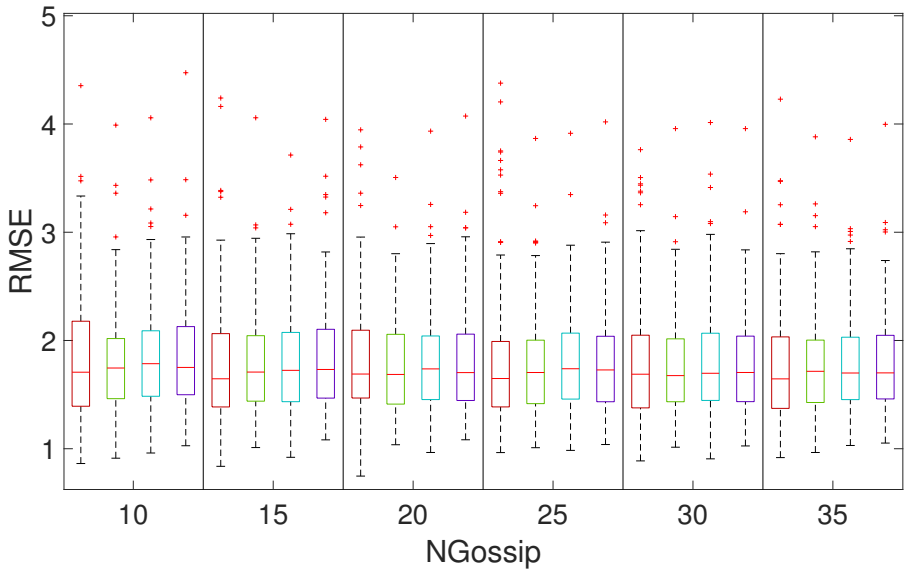

(a) RMSE

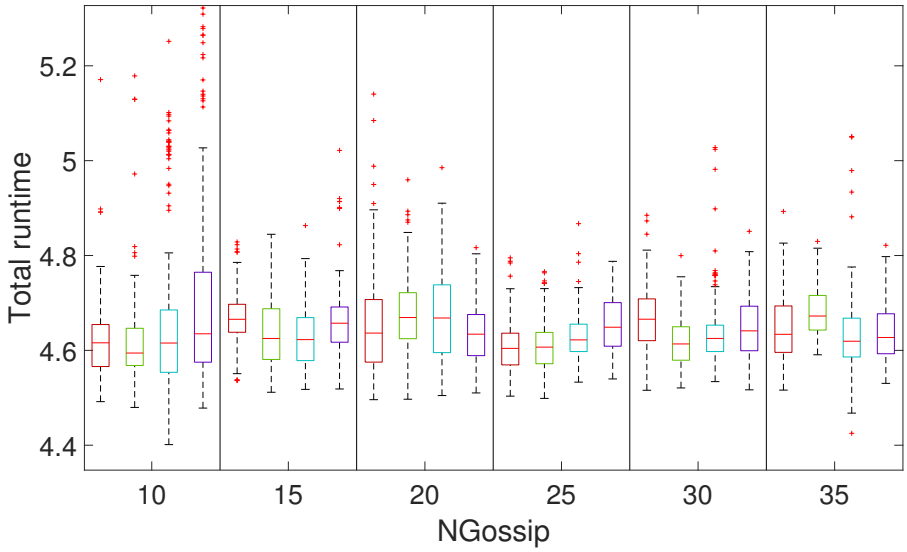

(b) total runtime

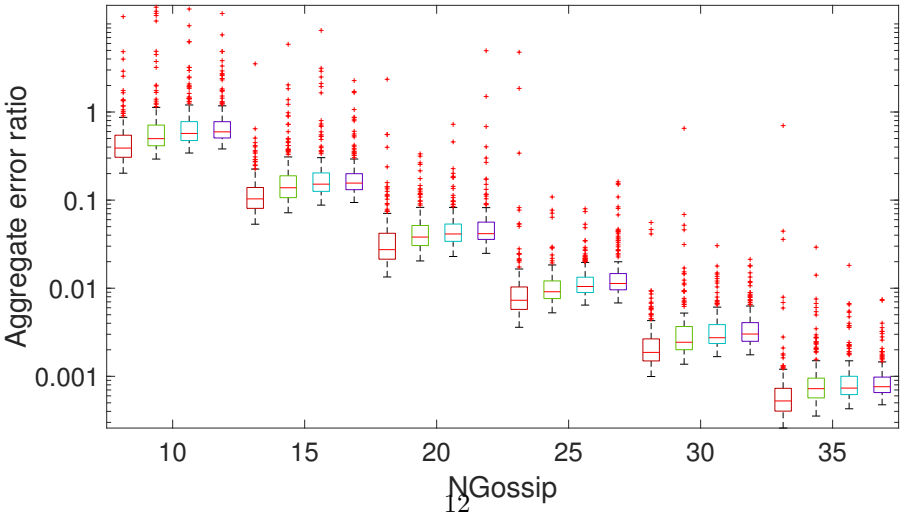

(c) total runtime

Figure 6: Boxplot of RMSE, runtime and aggregate error ratio of LApf with respect to $NGossip$ and m for 200 Monte Carlo trials ($N = 500$). For each value of $NGossip$, from left to right, $m = 6, 20, 50, 100$

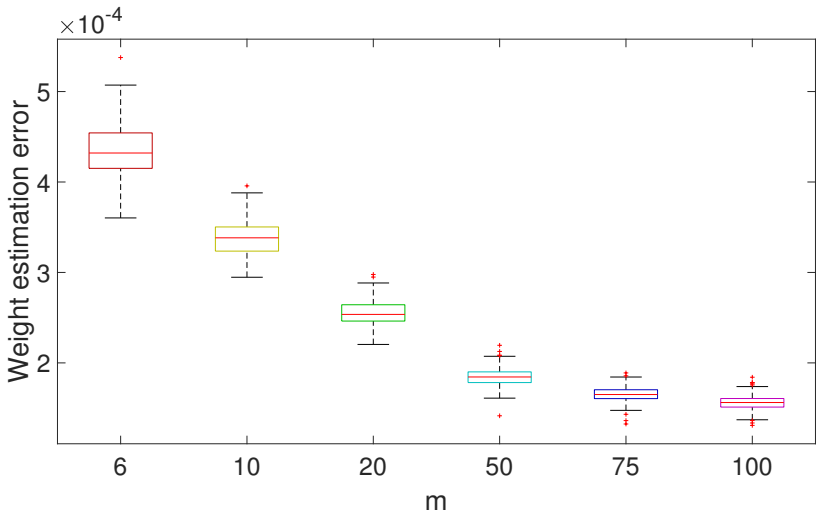

Figure 7: Boxplot of weight discrepancy with respect to m

	C = 6	10	20	50	100	200	500	1000
K = 3	7.2659	5.8947	4.9396	4.2876	3.5259	2.9242	2.1867	2.145
4	5.788	4.8958	4.2774	3.8178	3.6676	2.7393	2.1351	2.145
5	4.8997	4.3572	4.2338	3.6465	3.3935	2.6175	2.082	2.145
6	4.484	3.5367	3.4824	3.3628	2.9538	2.3805	2.2021	2.145
7	3.8512	3.8754	3.7534	3.2243	2.6819	2.2898	2.1499	2.145
8	3.9089	3.3702	3.3426	2.9276	2.5027	2.2326	2.1574	2.145
9	3.5868	3.1086	3.0701	2.8636	2.5661	2.2189	2.161	2.145
10	3.51	3.0733	2.919	2.4383	2.3067	2.1811	2.1323	2.145
20	2.4083	2.2209	2.2114	2.2414	2.2362	2.2464	2.1979	2.145
50	2.2432	2.2315	2.1922	2.274	2.2721	2.2163	2.2494	2.145
100	2.3841	2.2779	2.2087	2.1232	2.1998	2.2225	2.233	2.145

Table 1: RMSE of Clusterpf with respect to K and C over 100 Monte Carlo trials

	C = 6	10	20	50	100	200	500	1000
K = 3	7.5892	7.261	7.319	11.6321	19.1915	42.2104	194.2847	748.8655
4	5.3822	7.376	8.1377	10.3778	20.1636	41.0503	209.7392	745.8139
5	5.7585	7.7351	8.5754	11.9199	22.4751	41.4862	202.5959	737.2755
6	5.6528	6.1532	6.9711	12.2259	21.3191	47.8484	208.5728	731.9177
7	5.6642	6.2151	8.2362	13.5284	21.5673	45.5246	201.8637	735.6102
8	5.5074	7.2165	8.6544	13.8472	22.0559	46.9042	212.0588	752.7881
9	5.443	7.3545	8.7816	11.9092	20.5374	48.2595	205.2912	752.7088
10	5.47	7.4078	8.3934	13.7549	18.4591	46.0232	205.4603	742.8909
20	9.4839	8.0864	9.1319	13.1057	26.0044	42.5927	215.7453	773.2
50	9.2247	10.1492	11.2527	16.6921	24.2699	45.6228	205.8808	769.31
100	13.7989	13.2524	13.3149	23.1734	25.7608	54.9912	217.2478	766.9748

Table 2: Runtime of Clusterpf with respect to K and C over 100 Monte Carlo trials

to minimize the communication overhead without significantly degrading tracking performance. We note that CSSpf, LApf and Clusterpf have the same communication overhead (i.e., distributed aggregation of six

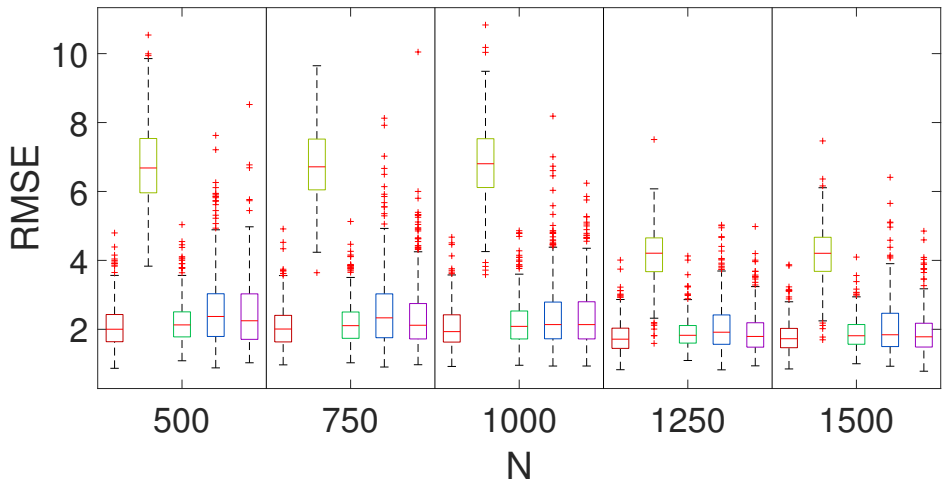

(a) Boxplot of RMSE

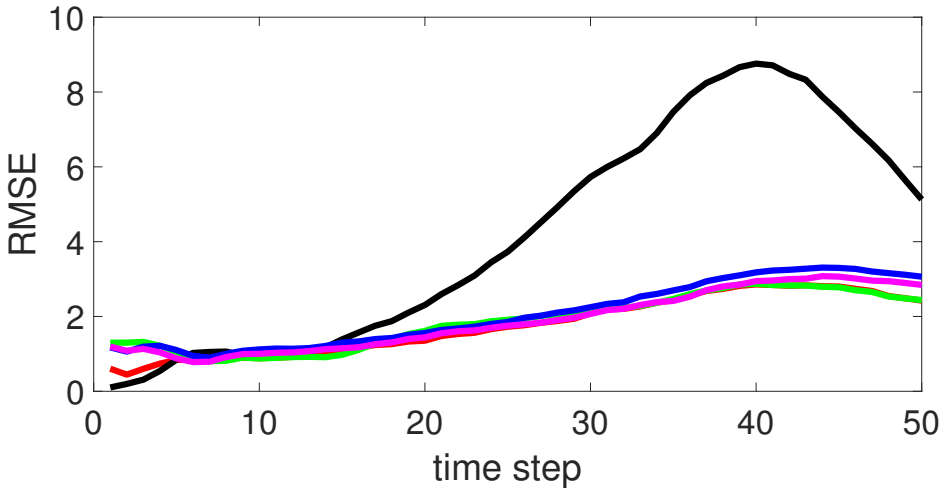

(b) time-averaged RMSE for $N = 1000$

Figure 8: RMSE comparison of all particle filters. For each value of N, from left to right: BSpf, CSSpf, LCpf, LApf, Clusterpf

statistics) whereas LCpf has a much higher overhead (i.e., aggregation of twenty scalars across sensors).

Fig. 8 shows the boxplot of RMSE with respect to N, the number of particles and the time-averaged RMSE for $N = 1000$. The CSSpf has the worst performance by a significant margin while the other four particle filters have similar performance and the performance of CSSpf starts degrading around time step $k = 15$. Fig. 9 shows the estimated trajectory of CSSpf from one trial and we can clearly see where the estimated track diverges from the true track. Table. 3 shows the average total runtime of all filters. BSpf, CSSpf and LCpf have similar runtime and are considerably faster than LApf and Clusterpf. The LApf has the longest runtime by far with the gap increasing at higher N which can be attributed to the eigenvalue decomposition.

In our next test, we shift the target trajectory and repeat the simulations. As Fig. 10 shows, all algorithms achieve lower RMSE compared to the first track. The CSSpf again has the highest RMSE; although the performance gap is considerably smaller. For all values of N, all other filters have similar performance. Fig. 11 shows the estimated trajectory of CSSpf for one random trial and the divergence between estimated and true tracks again occur around the outer corner turn. Table 4 shows the average runtime. Again, BSpf,

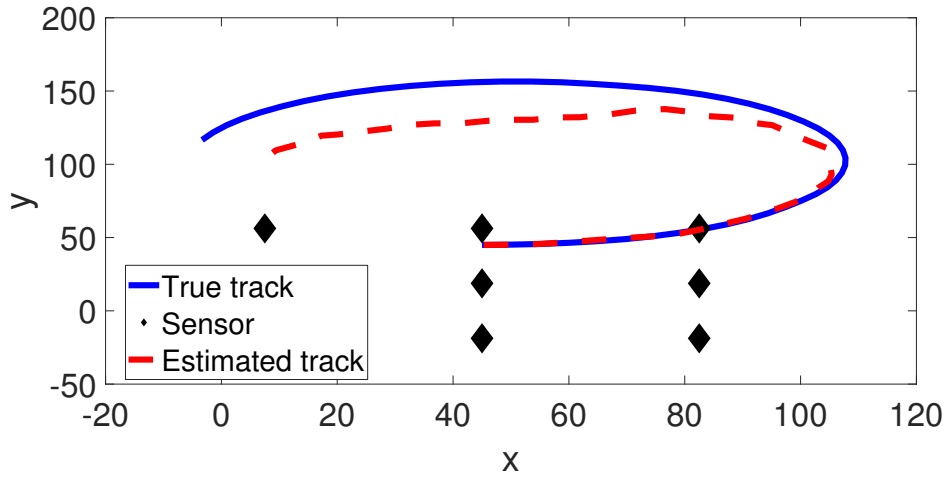

Figure 9: Estimated trajectory of CSSpf for one Monte Carlo trial at $N = 1000$

	N=500	N=750	N=1000	N=1250	N=1500
BSpf	0.2029	0.2425	0.2869	0.5624	0.5639
CSSpf	0.1265	0.1521	0.1825	0.6723	0.7253
LCpf	0.3053	0.3539	0.4112	0.7455	0.7796
LApf	7.6591	19.6260	39.5854	136.5413	247.4128
Clusterpf	5.0266	7.4632	10.4339	22.5435	29.3879

Table 3: Average total runtime of all filters with respect to N for 1st track

CSSpf and LCpf have similar short runtime while LApf has the highest runtime.

5 Conclusion

In this report, we present four distributed particle filters for single-target bearing-only tracking. CSSpf approximates the log-likelihood function using six sufficient statistics. LCpf uses likelihood consensus to approximate the measurement function. LApf constructs a graph over all particles and uses the eigenvectors of resulting Laplacian matrix to encode the particle log-likelihood. Finally, Clusterpf groups particles into clusters, computes the cluster joint log-likelihood and recovers individual particle weights using convex minimization.

We study each individual algorithm's performance and compare them against each other. CSSpf has the worst tracking performance by far. LCpf yields competitive tracking performance on-par with the centralized bootstrap particle filter and has very low runtime. On the other hand, it also has the highest communication overhead. LApf has very high runtime due to the computational overhead of eigenvalue decomposition

	N=500	N=750	N=1000	N=1250	N=1500
BSpf	0.2064	0.2495	0.3045	0.5407	0.5557
CSSpf	0.2649	0.3313	0.4012	0.6497	0.7179
LCpf	0.2947	0.3678	0.4372	0.7125	0.7657
LApf	7.7287	20.0299	41.4953	145.4905	265.9044
Clusterpf	5.0872	7.6359	10.9596	23.2325	31.8395

Table 4: Average total runtime of all filters with respect to N for 2nd track

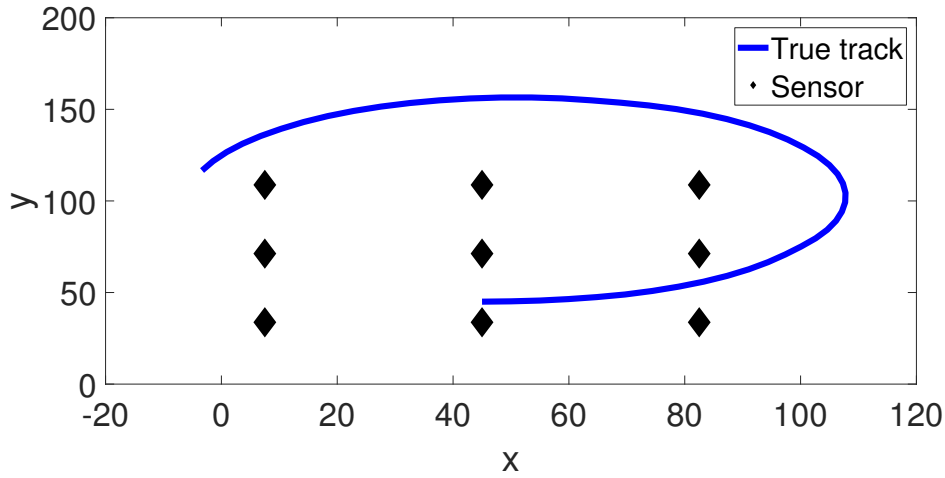

(a) Track

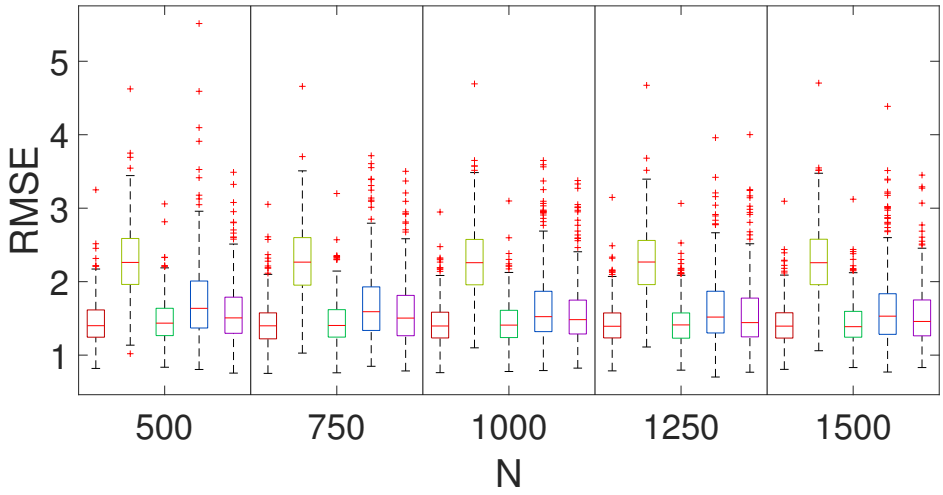

(b) RMSE

Figure 10: 2nd Test trajectory and boxplots of RMSE with respect to N. For each value of N, from left to right: BSpf, CSSpf, LCpf, LApf, Clusterpf

which renders it impractical for applications with strict timing constraints. Finally, Clusterpf has the second highest runtime but also yields competitive tracking performance.

References

[1] A. Mohammadi and A. Asif, "A constraint sufficient statistics based distributed particle filter for bearing only tracking," in *IEEE Int. Conf. Communications (ICC)*, Ottawa, ON, Canada, Jun 2012, pp. 3670–3675.

[2] O. Hlinka, O. Sluciak, F. Hlawatsch, P. Djuric, and M. Rupp, "Likelihood consensus and its application to distributed particle filtering," *IEEE Trans. Signal Process.*, vol. 60, no. 8, pp. 4334–4349, 2012.

[3] M. Rabbat, M. Coates, and S. Blouin, "Graph laplacian distributed particle filtering," in *Signal Process. Conf. (EUPISCO)*, Budapest, Hungary, Aug. 2016, pp. 1493 – 1497.

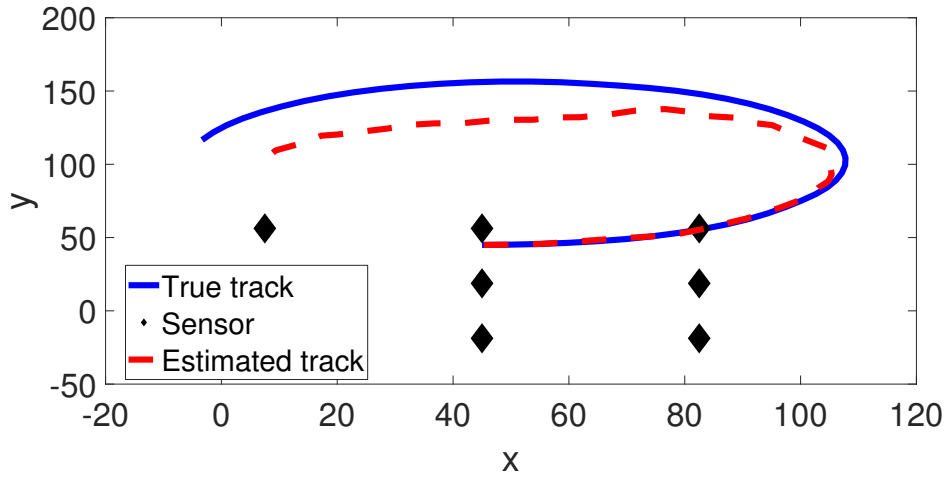

Figure 11: Estimated trajectory of CSSpf for one Monte Carlo trial at $N = 1000$

[4] C. W. Chao, M. Rabbat, and S. Blouin, "Particle weight approximation with clustering for gossip-based distributed particle filters," in *IEEE Int. Workshop Comp Comput. Advances Multi-Sensor Adaptive Process. (CAMSAP)*, Cancun, Mexico, Dec 2015, pp. 85–88.